Hydrogen Concentration and Mechanical Dissipation upon Annealing in Zirconia-doped Tantala Thin Films for Gravitational Wave Observatory Mirrors

A.W. Lussier[1], É. Lalande[1], M. Chicoine[1], C. Lévesque[1], S. Roorda[1], B. Baloukas[2], L. Martinu[2], G. Vajente[3], A. Ananyeva[3], F. Schiettekatte[1,*]

[1]Département de physique, Université de Montréal, Montréal, Québec, Canada
[2]Département de génie physique, Polytechnique Montréal, Montréal, Québec, Canada
[3]LIGO Laboratory, California Institute of Technology, Pasadena, CA, USA

*Corresponding author email: francois.schiettekatte@umontreal.ca

Abstract Sensitivity in instruments such as the Laser Interferometer Gravitational-Wave Observatory (LIGO) is limited by a noise originating from fluctuations linked to internal mechanical dissipation (IMD) in the amorphous thin films of their Bragg reflectors. We investigate the correlation between IMD, characterized by a loss angle, and the hydrogen concentration in a thin film made of Zr-doped tantalum oxide after annealing at different temperatures. The film was deposited by magnetron sputtering and the loss angle measured by gentle nodal suspension. The concentration of heavier elements was obtained by Rutherford backscattering spectrometry (RBS). The hydrogen concentration in the as-deposited and annealed samples was obtained by elastic recoil detection (ERD). We observe that the hydrogen atomic concentration gradually decreases from 2.0 ± 0.1% down to the detection limit at 0.2 ± 0.1% as we anneal to 650°C. We also find that the loss angle decreases by a factor of two over the same annealing temperature range, suggesting that the loss angle is correlated with the hydrogen concentration. However, the loss angle remains relatively high even when most of the hydrogen is desorbed. We conclude that the presence of hydrogen is not the main limiting factor for further reducing the IMD.

1. Context and Objectives

Gravitational wave detectors such as the Laser Interferometer Gravitational-Wave Observatory (LIGO) are based on a Michelson interferometer, equipped with a Fabry-Perot cavity in each of its arms, to measure with extreme precision the phase shift that originates from contractions and dilations of space following the propagation of a gravitational wave [1]. Since 2015, they have successfully detected the gravitational waves emitted by the fusion of several pairs of compact objects including neutron stars and black holes [2]. The test masses shown in Fig. 1 are equipped with Bragg mirrors made of alternating films of silica (SiO_2) and tantala (Ta_2O_5) doped with titania (TiO_2) deposited on fibre-suspended 40 kg silica substrates. There are multiple factors that affect the quality of the signal. The largest sources of noise in the most sensitive frequency range are the quantum noise [3], represented by the purple curve in Fig. 2, and the Brownian noise, represented by the red line, which results from the surface fluctuations of the amorphous films that compose the Bragg mirrors. An important reduction in the so-called

Brownian noise could considerably improve the sensitivity of the detector and lead to the detection of more gravitational wave events, and more precise signals to better understand their physics.

Through the dissipation-fluctuation theorem, the Brownian noise in the thin films is fundamentally linked to the internal mechanical dissipation, a feature of amorphous materials [4, 5]. This dissipation can then be characterized by a loss angle (reciprocal of the quality factor of an oscillator) which should be minimized to lower the noise. The internal dissipation in amorphous materials usually decreases upon thermal annealing as they structurally relax, in particular in the case of tantala [6]. Some doping elements such as Ti are found to decrease the loss angle or to frustrate its crystallization, allowing further annealing and relaxation [7]. However, impurities such as hydrogen are known to desorb from materials upon annealing, including ZrO_2 [8]. H is also known to passivate dangling bonds in many materials including Ta_2O_5 where it results, for example, in a decrease of the leakage current [9]. As it could also potentially affect the mechanical dissipation, we investigate the evolution of the H concentration as a function of the annealing temperature and its relationship with the loss angle in zirconia-doped tantala.

2. Experimental details

We studied zirconia-doped tantala layers that were part of a previous investigation; details about their properties and synthesis by magnetron sputtering (MS) at Polytechnique Montréal can be found in Ref. 6. We used two 75-mm-diameter Ta and Zr metallic targets subject to a radiofrequency bias, located about 25 cm from the sample holder. The base pressure in the preparation chamber was below 0.1 μtorr and a 30 sccm gas flow of 20% O_2 in Ar maintained the pressure at 5 mTorr during deposition.

The film was deposited on a silica disk substrate (75 mm diameter, 1 mm thick) located at the center of the sample holder for subsequent loss angle measurements. In addition, for the H analysis presented here, we simultaneously deposited the film on a c-Si witness substrate located on the side of the sample holder.

We measured the loss angle of the main as-deposited sample, and then we thermally annealed it for 10 hours in air at 400°C, 500°C, 600°C and 650°C at CalTech. The loss angle was measured by Gentle Nodal Suspension (GeNS) [10] between each annealing steps. In GeNS, we electrostatically excite the vibrational modes of the disk which rests centered on a spherical surface, and we extract the loss angle from the amplitude decay. We note that the sample annealed at 650°C showed signs of crystallization. [6]

The witness sample was cut into 4 pieces, and three of these parts were subject to similar thermal treatments where they were annealed for 15 h in air at 400°C, 500°C and 650°C, respectively. Note that these samples were annealed separately from each other while the main silica disk sample underwent each annealing step in sequence.

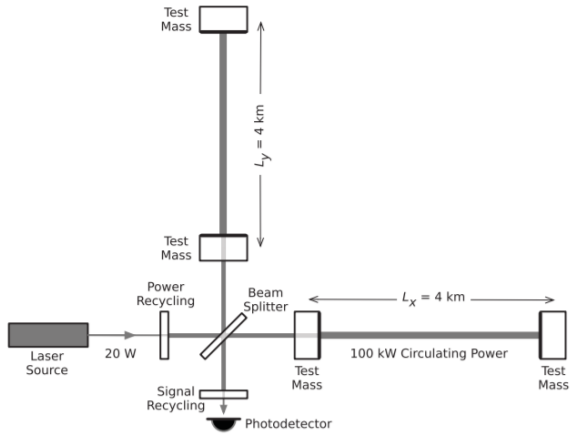

Fig. 1. Schematic of the LIGO interferometer (adapted from Ref. [2]).

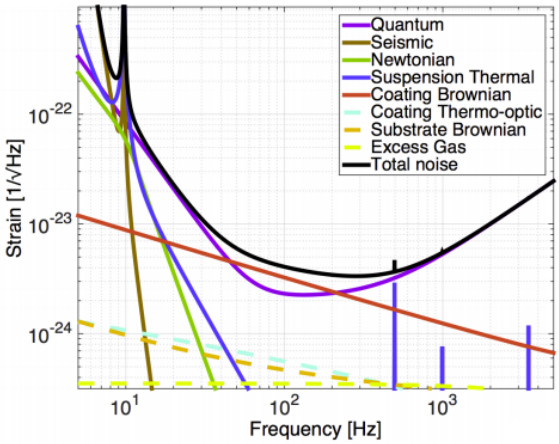

Fig. 2. Contributions to the noise level in the LIGO experiment. From Ref. [11].

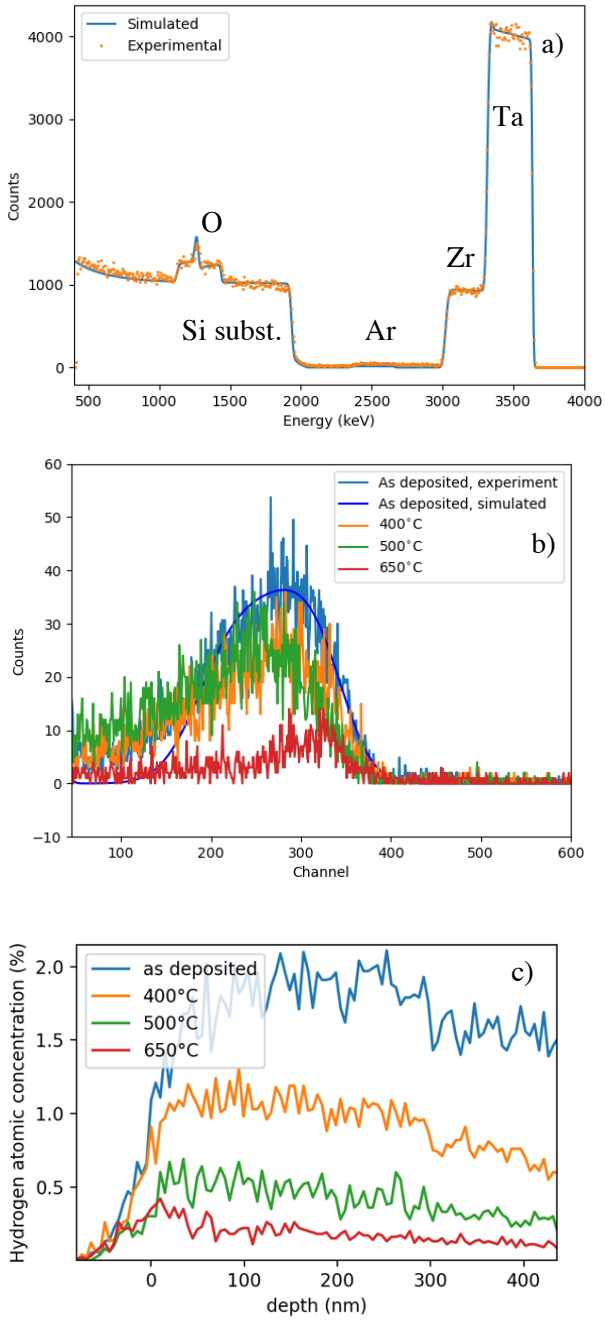

Fig. 3. a) RBS spectrum of the as-deposited sample obtained with ^{4}He 4 MeV beam at 7° incidence from surface normal. (b) Hydrogen ERD spectra obtained with a 4.1 MeV ^{4}He at 75° incidence, and (c) depth profiles obtained with a 35 MeV ^{35}Cl beam from samples as-deposited or annealed at indicated temperatures.

In order to relate the loss angle measured on the main sample to the hydrogen concentration measured on the witness samples, we performed ion beam analysis on the latter. First, we measured the heavy atom depth profile in the film by Rutherford backscattering spectrometry (RBS) [12] with a ^{4}He beam of 4 MeV ions at a backscattering angle of 170°. As seen in Fig. 3a, this energy and geometry allowed to a good mass resolution. An incidence angle of 7° with respect to the surface normal was selected to minimize channeling through the *c*-Si substrate.

Subsequently, we measured the H concentration of each piece by elastic recoil detection (ERD) [13] using two different setups. First, we acquired each ERD spectrum while simultaneously measuring an RBS spectrum. The beam used was a 4.1 MeV ^{4}He. For the ERD part of this measurement, the angle of incidence with respect to the surface normal was 75° and the recoil angle was 40°, with an exit angle of 65°. We used a 20.3 μm thick Mylar absorber in front of the ERD to filter the He atoms but let through the H atoms. The spectra are shown in Fig. 3b. For the RBS part of this measurement, the detector was placed at a recoil angle of 130° and an exit angle of 25°. From the RBS spectra, we can obtain a reference for the product of the incident particles and the solid angle from the substrate signal. Knowing the solid angle of both ERD and RBS detectors, this product allows us to quantify how the amplitude of the ERD measurement relates to the hydrogen concentration.

As a next step, we measured an H depth profile using ERD while simultaneously carrying out ERD-time-of-flight (ERD-TOF) [14] measurements for the heavier elements using a 35 MeV ^{35}Cl beam. [15] In that case, the beam angle of incidence was 75° with respect to the surface normal and, for the H measurement, the recoil angle was 46°, corresponding to an exit angle of 59°. In front of the ERD detector was a 12.7 μm-thick Mylar foil to filter out the scattered Cl atoms. The ERD-TOF detector was at a recoil angle of 30°

so the exit angle was 75°. The H concentration was established in relation to the O content measured by the ERD-TOF.

The He beam measurements allow one to obtain a spectrum that covers the complete layer thickness while the Cl beam measurements offer a better depth resolution, but a shallower probing depth (see Fig. 3b and c, respectively). We used the software SIMNRA [16] to simulate both RBS and ERD spectra obtained with the He beam at 4 MeV and 4.1 MeV to obtain the atomic concentrations of each element contained in the sample, assuming a uniform slab for the coating. The H spectra obtained with the 35 MeV Cl beam were converted into depth profiles using the Allegria software, which iteratively performs an energy-to-depth conversion of the energy spectra of each mass by computing the stopping power based on the Bragg rule from the previous iteration [17].

3. Results and discussion

For the as-deposited sample, the simulation of the RBS measurement (Fig. 3a) shows that the layer consists of a uniform atomic concentration of 12.5 ± 1% of Zr, 16.5 ± 1% of Ta, 68 ± 2% of O, and 1.0 ± 0.2% of Ar. In Fig. 3c, we can see from the measurement with a 35 MeV Cl beam that this layer also contains 1.9 ± 0.2% of H on average, at least in the top part of the film. The decrease with depth might be the result of an imperfect knowledge of the stopping power of the various atoms at play in this compound layer. A simulation of the ERD spectrum obtained with the 4.1 MeV He beam for the as-deposited sample, shown in Fig. 3b, gives a value of 2.0 ± 0.1% of H. Most coatings produced for the experiments described in Ref. 6 and other similar experiments have a hydrogen concentration of 1.5% to 3.5%, so hydrogen impurities seem to be commonplace. Since no H-containing molecules are deliberately injected in the chamber during the deposition, we surmise that they come from water vapor desorbing from the chamber walls or from the exposure of the samples to the atmosphere after the film deposition. According to the simulation in Fig. 3a, the film has an areal atomic concentration of H of $(4.13\pm0.05) \times 10^{18}$ at/cm^2. Considering a density of 6.6 ± 0.2 g/cm^3 [6], its resulting calculated thickness is 530 ± 20 nm. This is about 13% thinner than the thickness of the film on the main silica disk of about 614 nm measured by ellipsometry. The reason for this is that the witness sample was placed on the outskirts of the sample holder while the main sample was in its center receiving a higher flux of condensing particles during deposition.

Upon annealing, the ERD measurements (Fig. 3b and c) show a clear decrease in the H concentration as a function of annealing temperature. H surface peaks cannot be distinguished in any of the measurements aside from the sample annealed at 650°C; indeed, it is visible near channel 350 in Fig. 3b, and is comparatively more intense than for the corresponding sample at the origin of Fig. 3c. As mentioned, the ERD measurement with the 4.1 MeV ^{4}He beam has a deeper probing depth of about 1 μm thus covering the whole 530 nm of the film, whereas the depth probed in Fig. 3c covers about 4/5 of the film thickness. However, we see that the 4.1 MeV ^{4}He measurement offers a poor depth resolution due to the geometrical straggling that originates from the detector's large solid angle, and the small stopping power of He, in comparison to Cl.

In Fig. 4a, we compare the two sets of H concentration measurements as a function of the annealing temperature. The as-deposited sample contains about 2% of hydrogen as previously mentioned, while after annealing at 650°C, the hydrogen concentration has decreased by a factor of 10. For intermediate temperatures, the results slightly differ, the measurement carried out with the He beam giving a higher H content. One might consider that this is due to beam-induced H desorption, which is typically more prominent with heavier atoms [18].

In comparison, during the 35 MeV ^{35}Cl measurements, the H counting rate remained the same as that of the other atoms. Therefore, we did not observe any desorption during these measurements. We also note that the amount of H is small, which usually limits desorption, which is often a bimolecular process. According to our results, hydrogen desorbs at a regular rate with temperature, and the process does not seem to be characterized by a single activation energy.

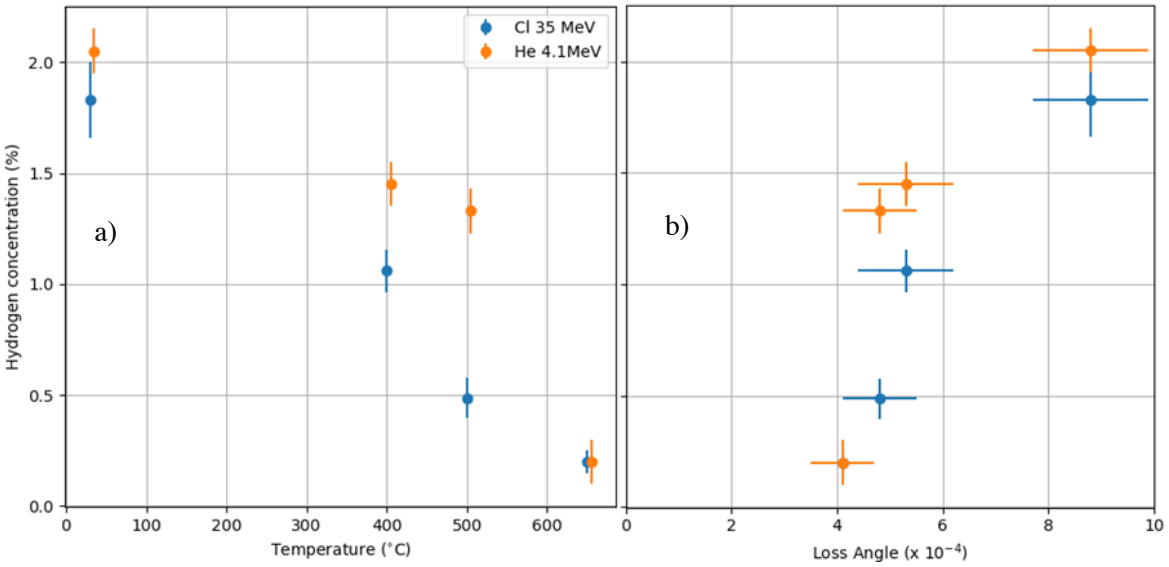

Fig. 4. a) Average H concentration in the film as a function of the annealing temperature as obtained with the two different beams. b) Average H concentration as a function of the loss angle.

Then, by relating the loss angles measured on the main sample to the measured H concentration in the witness samples, we obtain Fig. 4b. The hydrogen concentration is seen to decrease down to the detection limit with annealing temperature while the loss angle decreases by about half and remains relatively high at around 4×10^{-4} even if most of the hydrogen has already been extracted. This leads us to conclude that hydrogen is not the main factor in the internal mechanical dissipation. Although Fig. 4b may seem to indicate that there is a correlation between the hydrogen content and the loss angle, this does not imply a causal relationship; indeed, they might just be two simultaneously thermally activated processes: H desorption and structural relaxation, the latter one having already been identified in amorphous zirconia-doped tantala [19]. Finally, as previously mentioned, the main sample (used for loss angle measurements) and the witness samples (used for H concentration measurement) differed in their annealing time (10 h vs. 15 h) and the fact that the main sample was sequentially annealed multiple times. If anything, more H should have been desorbed from the main sample than the witness sample pieces, thus showing that H content is not the limiting factor to lower the loss angle under 4×10^{-4}.

4. Conclusion

We have used ERD in a variety of geometries to measure the hydrogen concentration and its depth profile in Zr-doped Ta_2O_5 annealed at 400°C, 500°C and 650°C. We found a hydrogen concentration of 2.0 ± 0.1% in the as-deposited sample, and have observed a regular decrease of the hydrogen concentration as the annealing temperature was increased, reaching 0.2 ± 0.1% after an anneal at 650°C. We have also observed a correlation between the H concentration and the internal mechanical dissipation in the film, but the latter is likely due to both the H desorption and the amorphous material's structural relaxation being thermally activated. Since the loss angle remains relatively high even when most of the hydrogen has been desorbed, we conclude that the presence of hydrogen is not the main limiting factor for further reducing the loss angle.

However, the role of H in the material, whether it passivates dangling bonds or is simply trapped, needs to be investigated further using techniques such as X-ray photoelectron spectroscopy and/or infrared spectroscopy. It could also be interesting to verify the effect of deliberate H doping on the loss angle to see if our conclusion holds. Numerical simulations would also be of great interest to better understand the effect of hydrogen on the mechanical properties of amorphous materials.

Acknowledgments

The work performed at U. Montréal and Polytechnique Montréal was supported by the Natural Sciences and Engineering Research Council of Canada (NSERC), the Canadian foundation for innovation (CFI) and the Fonds de recherche Québec, Nature et technologies (FQRNT) through the Regroupement Québécois sur les matériaux de pointe (RQMP). The authors thank F. Debris and L. Godbout from U.

Montréal and F. Turcot from Polytechnique Montréal for their technical assistance. They also thank their colleagues within the LIGO Scientific Collaboration for advice and support. LIGO was constructed by the California Institute of Technology and Massachusetts Institute of Technology with funding from the National Science Foundation, and operates under cooperative agreement PHY-0757058. Advanced LIGO was built under award PHY- 0823459. This paper has LIGO document number LIGO-P2100455.

References

[1] The LIGO Scientific Collaboration *et al*. Class. Quantum Grav. **32**, 074001 (2015)
[2] B. P. Abbott *et al*. (LIGO Scientific Collaboration and Virgo Collaboration) Phys. Rev. Lett. **116**, 061102 (2016).
[3] M. Tse *et al*. Phys. Rev. Lett. **123**, 231107 (2019).
[4] H. B. Callen and R. F. Greene, Phys. Rev. **86**, 702 (1952).
[5] Yu. Levin, Phys. Rev. **D 57**, 659 (1998).
[6] M. Abernathy *et al*. Class. Quantum Grav. 38 195021 (2021).
[7] É. Lalande, A.W. Lussier, C. Lévesque, M. Ward, B. Baloukas, L. Martinu, G. Vajente, G Billingsley, A. Ananyeva, R. Bassiri, M.M. Fejer, F. Schiettekatte, J. Vac. Sci. Technol. **A39**, 043416 (2021).
[8] S. Yamanaka, T. Nishizaki, M. Uno, M. Katsura, J. Alloys Compd., 293–295, 38 (1999).
[9] W.S. Lau, K.K. Khaw, Appl. Phys. Lett. 89, 262901 (2006).
[10] G. Vajente, A. Ananyeva, G. Billingsley, E. Gustafson, A. Heptonstall, E. Sanchez, C. Torrie, Rev. Sci. Instrum. **88**, 073901 (2017).
[11] L. Barsotti, S. Gras, M.Evans, P. Fritschel, *The updated Advanced LIGO design curve,* Technical Note LIGO-T1800044-v5 (2018).
[12] *Backscattering Spectrometry*, W.-K. Chu, J.W. Mayer, M.-A. Nicolet, Academic Press, 1978
[13] J. L'Ecuyer, C. Brassard, C. Cardinal, J. Chabbal, L. Deschênes, J.P. Labrie, B. Terreault, J.G. Martel, R. St-Jacques, J. App. Phys. **47** (1976) 381.
[14] M. Chicoine, F. Schiettekatte, M.I. Laitinen, T. Sajavaara, Nucl. Intrum. Meth. **B 406** (2017) 112
[15] On our setup, the H detection efficiency by the TOF camera is only a few percent and may change in time, so more reliable measurements are obtained by standard ERD.
[16] M. Mayer, AIP Conference Proceedings **475**, 6 (1999).
[17] F. Schiettekatte, M. Chicoine, S. Gujrathi, P. Wei, K. Oxorn, Nucl. Inst. Meth. **B 219-220,** 125 (2004).
[18] F. Schiettekatte, A. Chevarier, N. Chevarier, A. Plantier, G.G. Ross, Nucl. Instr. Meth. **B132**, 607 (1997).
[19] K. Prasai, J. Jiang, A. Mishkin, B. Shyam, S. Angelova, R. Birney, D. A. Drabold, M. Fazio, E. K. Gustafson, G. Harry, S. Hoback, J. Hough, C. Lévesque, I. MacLaren, A. Markosyan, I. W. Martin, C. S. Menoni, P. G. Murray, S. Penn, S. Reid, R. Robie, S. Rowan, F. Schiettekatte, R. Shink, A. Turner, G. Vajente, H-P. Cheng, M. M. Fejer, A. Mehta, R. Bassiri, Phys. Rev. Lett. **123** (2019) 045501.